Journal of Materials Chemistry A

Electrospun MXene/Carbon Nanofibers as Supercapacitor Electrodes

Journal:	*Journal of Materials Chemistry A*
Manuscript ID	TA-ART-10-2018-009810.R2
Article Type:	Paper
Date Submitted by the Author:	21-Nov-2018
Complete List of Authors:	Levitt, Ariana; A.J. Drexel Nanomaterials Institute, Drexel University, Materials Science and Engineering; Center for Functional Fabrics, Drexel Univeristy Alhabeb, Mohamed; A.J. Drexel Nanomaterials Institute, Drexel University, Materials Science and Engineering Hatter, Christine; A.J. Drexel Nanomaterials Institute, Drexel University, Materials Science and Engineering Sarycheva, Asia; A.J. Drexel Nanomaterials Institute, Drexel University, Materials Science and Engineering Dion, Genevieve; Center for Functional Fabrics, Drexel University Gogotsi, Yury; A.J. Drexel Nanomaterials Institute, Drexel University, Materials Science and Engineering

Journal of Materials Chemistry A

PAPER

Electrospun MXene/Carbon Nanofibers as Supercapacitor Electrodes

Received
Accepted

DOI:

www.rsc.org/

Ariana S. Levitt,[ab] Mohamed Alhabeb,[a] Christine B. Hatter,[a] Asia Sarycheva,[a] Genevieve Dion,[b] Yury Gogotsi*[a]

Free-standing $Ti_3C_2T_x$ MXene/carbon nanofiber electrodes are prepared *via* electrospinning $Ti_3C_2T_x$ MXene flakes with polyacrylonitrile (PAN) and carbonizing the fiber networks. Using this simple fabrication method, delaminated MXene flakes are embedded within carbon nanofibers and these fiber mats are used as electrodes without binders or additives. Unlike coated electrodes, which may suffer from the active material delaminating from the substrate during folding or bending, composite electrodes are stable and durable. Previous attempts to incorporate $Ti_3C_2T_x$ MXene into electrospun fibers resulted in low mass loadings, ~1 wt.% $Ti_3C_2T_x$ MXene. In this work, MXene flakes are added into PAN solutions at a weight ratio of 2:1 (MXene:PAN) in the spinning dope, producing fiber mats with up to 35 wt.% MXene. Composite electrodes have high areal capacitance, up to 205 mF cm^{-2} at 50 mV s^{-1}, almost three times that of pure carbonized PAN nanofibers (70 mF cm^{-2} at 50 mV s^{-1}). Compared with electrospun nanofibers spray-coated with $Ti_3C_2T_x$, these composite fibers exhibit double the areal capacitance at 10 mV/s. This method can be used to produce MXene composite fibers using a variety of polymers, which have potential applications beyond energy storage, including filtration, adsorption, and electrocatalysis, where fibers with high aspect ratio, accessible surface, and porosity are desirable.

1 Introduction

Due to the excellent conductivity (up to 10,000 S/cm as a freestanding film),[1] high electrochemical activity,[2] and high specific surface area of 2D transition metal carbides and nitrides (MXenes), there is much interest in developing MXene fibers for smart textile applications. These applications include energy storage devices for powering wearable electronics, energy harvesting devices for generating power, and wearable antennas for wireless communication. MXenes are a large family of two-dimensional transition metal carbides and nitrides with the general formula $M_{n+1}X_nT_x$, where M is an early transition metal, X is carbon and/or nitrogen and T_x is surface functional termination such as –OH, –F, –O.[1,3] As a result of their surface terminations, MXenes are hydrophilic and can easily form stable colloidal solutions for processing into various architectures.[1,4-6] For instance, $Ti_3C_2T_x$ MXene, the most studied material in the family to date, is commonly used as a free-standing film, power, coating, or ink for applications including energy storage,[2] electromagnetic interference (EMI) shielding,[7] and optoelectronics,[8] amongst others.

Recently, several works have been published on coating $Ti_3C_2T_x$ MXene onto fibers for wearable energy storage applications.[9,10] However, there are two main challenges associated with using coated fibers for this application. First, twisting, bending, knitting, and weaving often lead to the active material flaking off from the fiber, resulting in a decrease in conductivity. Second, increasing active mass loading often leads to restacking of MXene sheets, hindering the diffusion of ions and reducing electrochemical performance. As such, there is interest in embedding MXene flakes into fibers and forming integrated MXene fiber composites. To the best of our knowledge, only three works have been published on this topic to date.[11-13]

Fiber processing methods commonly used to incorporate nanomaterials into nano- and micro-scale fibers include wet-spinning, electrospinning, and melt-spinning.[14-19] These methods have their own merits, producing fibers of various architectures (core-shell, bi-

[a] A.J. Drexel Nanomaterials Institute and Department of Materials Science and Engineering, Drexel University, 3141 Chestnut St, Philadelphia, PA 19104, USA. E-mail: Gogotsi@drexel.edu
[b] Center for Functional Fabrics, Drexel University, 3141 Chestnut St, Philadelphia, PA 19104, USA

Electronic Supplementary Information (ESI) available: MXene flake size distribution, elemental analysis of electrospun fibers, rate handling plots of fiber electrodes. See DOI:

lobal, composite, etc.) with different properties. Electrospinning is a simple, versatile, and cost-effective method for producing nonwoven mats of nanoscale fibers and has been used extensively to incorporate nanomaterials into fibers with tunable properties, such as fiber diameter and fiber orientation.[20,21] These free-standing composite nanofibers are attractive for energy storage applications, as their high specific surface area can be used to promote ion adsorption and their porosity allows easy access of electrolyte ions. However, one of the challenges of electrospinning composite solutions containing particles or two-dimensional materials is that agglomeration or restacking of sheets may cause beading or inconsistencies across the fiber mat. Thus, it is critical to achieve a stable homogenous solution for electrospinning, which is essential for large scale device fabrication, such as supercapacitors.

Supercapacitors (SCs) are promising energy storage devices for wearable applications, as they have a long cycle life and can be made using non-toxic materials.[22] There are two categories of SCs: electrical double layer capacitors (EDLCs) and pseudocapacitors, and they differ by their energy storage mechanisms.[23] EDLCs store charge through the adsorption of ions on the surface of the electrode material, whereas pseudocapacitors store charge through fast redox reactions. Polyacrylonitrile (PAN), a carbon-precursor, is one of the most common polymers used in electrospinning to prepare electrodes for EDLCs due to its high carbon yield and ease of spinning.[24] However, the capacitive performance of pure PAN-derived carbon nanofibers (CNFs) is limited. By adding capacitive carbon materials, like graphene and carbon nanotubes, and pseudocapacitive transition metal oxides,[25] such as MnO_2, to the spinning dope, researchers have developed electrospun PAN composite nanofibers with enhanced electrochemical performance. For instance, Zhou *et al.* produced electrospun graphene/CNFs and the capacitance retention improved with the addition of graphene relative to pure CNFs.[19] $Ti_3C_2T_x$ MXene offers a higher conductivity than MnO_2 and many other pseudocapacitve materials and thus is a promising candidate for improving the electrochemical performance of carbon nanofibers. To our knowledge, only two studies have been published on electrospinning MXene, and both works resulted in low MXene loading (<1 wt.% in solution),[12,13] which is not sufficient for supercapacitor applications.

In this work, electrospinning is used as a simple method to embed $Ti_3C_2T_x$ MXene within carbon nanofibers. Flexible nonwoven mats of nanofibers are produced with up to 35 wt.% $Ti_3C_2T_x$ and the structure of $Ti_3C_2T_x$ MXene is maintained during the carbonization treatment. These freestanding electrospun mats are used as electrodes in supercapacitors, demonstrating enhanced electrochemical performance relative to pure carbon nanofibers.

2 Results and Discussion

2.1 Preparation of electrospinning solution

The schematic representation shown in Figure 1 illustrates the process of electrospinning $Ti_3C_2T_x$ MXene/PAN nanofibers and subsequently carbonizing PAN to produce MXene/carbon composite fibers. Prior to introducing MXene into the electrospinning solution, experiments were conducted to determine the minimum concentration of PAN needed to form homogenous, bead-free fibers, and 8 wt.% PAN was chosen for this work. DMF was selected as the solvent for preparing $Ti_3C_2T_x$ MXene/PAN solutions because DMF is commonly used for electrospinning pure PAN fibers due to its high vapor pressure and it has been previously demonstrated that $Ti_3C_2T_x$ MXene disperses well in

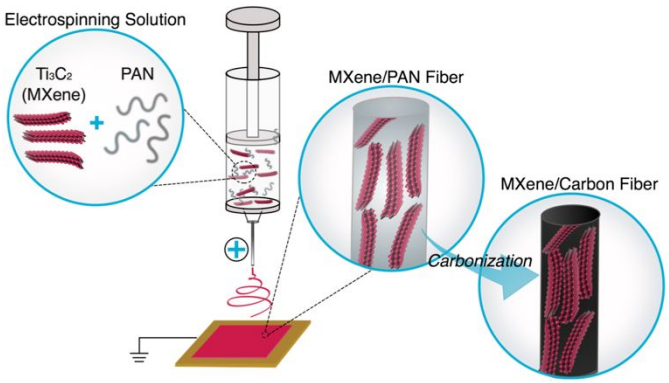

Fig. 1 Schematic of the production of $Ti_3C_2T_x$ MXene/carbon nanofibers *via* electrospinning. MXene/PAN solutions were prepared by dispersing delaminated MXene flakes in DMF and mixing with PAN. The solution was loaded into a syringe capped with a needle. A high voltage was applied to the needle tip and a nonwoven mat of MXene/PAN composite fibers was collected on a stationary copper plate. The fibers were stabilized and carbonized to form MXene/carbon nanofibers.

DMF.[26] As shown in Figure S1, solutions of MXene/PAN in DMF were homogenous after stirring at room temperature overnight, and films produced *via* vacuum-assisted filtration (VAF) show a layered morphology. It should be noted that the conductivity of $Ti_3C_2T_x$ MXene was greatly reduced after dispersing in DMF, likely due to the suppression of inter-flake electron hopping when large molecules intercalate between layers of MXene flakes.[27,28] For future work, other organic solvents with smaller molecular diameters, such as ethanol, should be considered for electrospinning MXene.

Prior to electrospinning, $Ti_3C_2T_x$ flakes were probe sonicated to produce monodisperse colloidal solutions with flake sizes similar to the diameter of pure PAN fibers, which range from 150-300 nm. Before sonication, as-synthesized $Ti_3C_2T_x$ MXene flakes were polydisperse, with flake sizes ranging from 100 nm up to 8 μm. After probe sonication, dynamic light scattering (DLS) showed that the lateral dimension of 80% of MXene flakes in DMF was approximately 300 nm. These values are in agreement with TEM observations (Figure S2).

2.2 Composition and morphology of electrospun MXene/PAN fibers

$Ti_3C_2T_x$ MXene composite fibers were successfully electrospun with up to 16 wt.% MXene in the electrospinning solution, as shown in Figure 2. No beading was observed across the fiber mats. The mats are freestanding (Figure 3A) and easily wrapped around a tube, demonstrating their flexibility (Figure 3B). Between 0 to 16 wt.% MXene, there is a gradual change in the color of the resulting electrospun mats, from a white fiber mat produced from 0 wt.% MXene solutions, to a black mat produced from 10 and 16 wt.% $Ti_3C_2T_x$ MXene solutions (Figure 3A).

As shown in Figure 2F, the average fiber diameter increased as a function of $Ti_3C_2T_x$ MXene concentration, from 179±33 nm to 958±190 nm for pure PAN fibers and 16 wt.% $Ti_3C_2T_x$ MXene fibers, respectively. SEM images reveal that at lower $Ti_3C_2T_x$ MXene concentrations, the fibers are less uniform with MXene flakes protruding from the fiber surfaces (Figure 2B). At higher MXene concentrations (16 wt.%), MXene flakes are interconnected along the fiber axis, increasing the

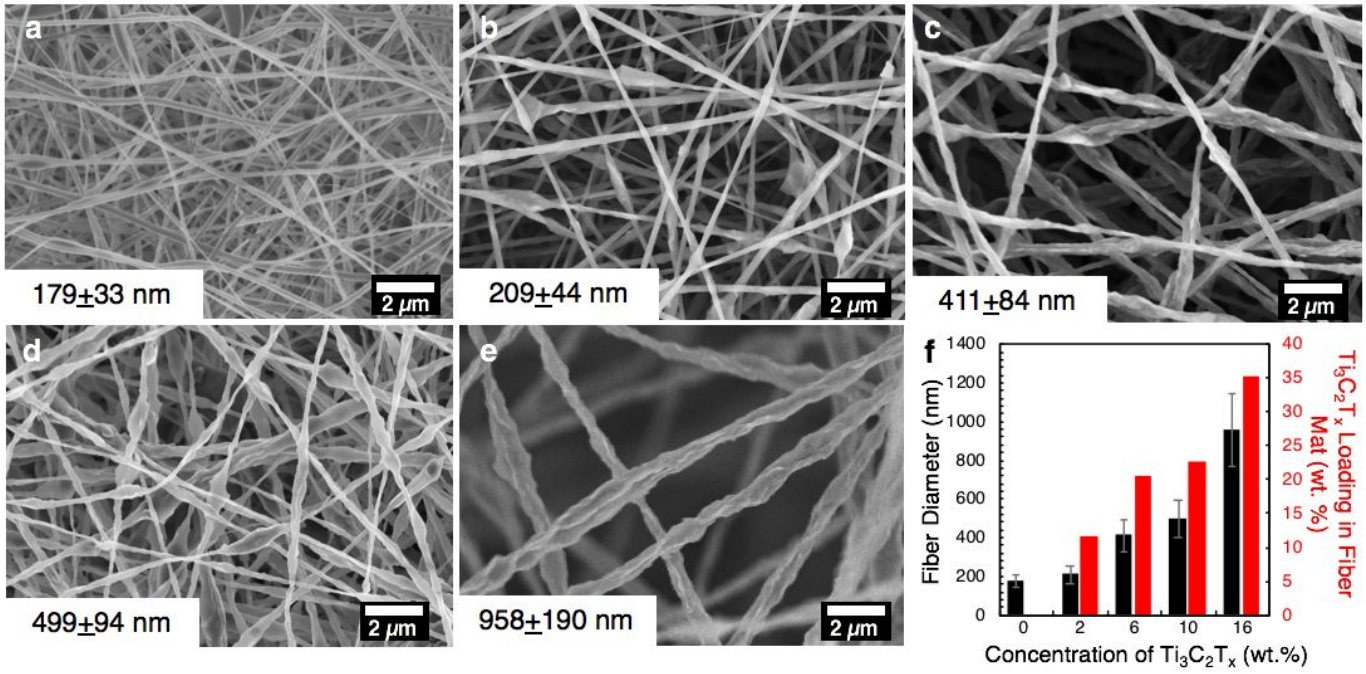

Fig. 2 Morphology of electrospun $Ti_3C_2T_x$ MXene/PAN fibers. SEM images of electrospun PAN fibers with increasing concentration of $Ti_3C_2T_x$ MXene in the electrospinning solution: a) 0 wt.%, b) 2 wt.%, c) 6 wt.%, d) 10 wt.%, e) 16 wt.%; f) bar chart of average fiber diameters and approximate loading of MXene in the fiber mats.

fiber diameter and uniformity. At 16 wt.%, as-spun MXene/PAN composite fibers are highly resistive, showing resistance values in MΩ. Beyond 16 wt.% $Ti_3C_2T_x$ MXene in the spinning solution, fibers started to stand up off of the collector plate. This phenomenon is often seen when electrospinning conducting materials, like intrinsically conducting polymers. When electrospinning conducting solutions, excess charges in the polymer jet dissipate quickly to the collector plate, inducing opposite chargers to the collector and resulting in fiber lift-off.[29]

The fiber morphology was further investigated using TEM. As shown in Figure 3C-E, single to few layers of $Ti_3C_2T_x$ MXene flakes are present inside of the fibers. The flakes are shown to be well aligned with the fiber axis (Figure 3D). Elemental analysis was conducted on fibers electrospun from a solution of 10 wt.% $Ti_3C_2T_x$ MXene and 8 wt.% PAN using energy-dispersive spectroscopy (EDS). EDS confirmed the presence of Ti in the fibers (Table S1). X-ray diffraction (XRD) patterns of the as-spun MXene/PAN fibers (10 wt.% MXene) show the (00*l*) peaks of $Ti_3C_2T_x$ MXene (Figure 4A). There is no significant shift in the (00*l*) peaks between the electrospun fiber mat and a free-standing film of $Ti_3C_2T_x$ MXene prepared by vacuum-assisted filtration (VAF) of a $Ti_3C_2T_x$ MXene/DMF solution. For example, the (002) peak is centered at 2θ of 6.70° and 6.63° for the fibers and film, respectively. This indicates that the spacing between MXene layers is relatively unchanged, despite mixing with PAN. Raman spectra of the as-spun fiber mats (Figure 4C) show a peak at 208 cm^{-1}, which is observed in Ti_3C_2 MXene and is attributed to Ti, C and O A_{1g} vibrations of oxygen-terminated Ti_3C_2.[30]

The thermal stability of the as-spun fiber mats was analyzed for mats produced with 0-16 wt.% MXene in the spinning solution (Figure 4B). A free-standing film prepared by VAF was analyzed for comparison. The fiber samples lost up to 10% of their weight before 200 °C, which can be attributed to the loss of water and DMF in the $Ti_3C_2T_x$ interlayers and removal of the $Ti_3C_2T_x$ surface functional groups.[9,31,32] The thermal decomposition temperature of PAN increased by approximately 35 °C with the inclusion of $Ti_3C_2T_x$

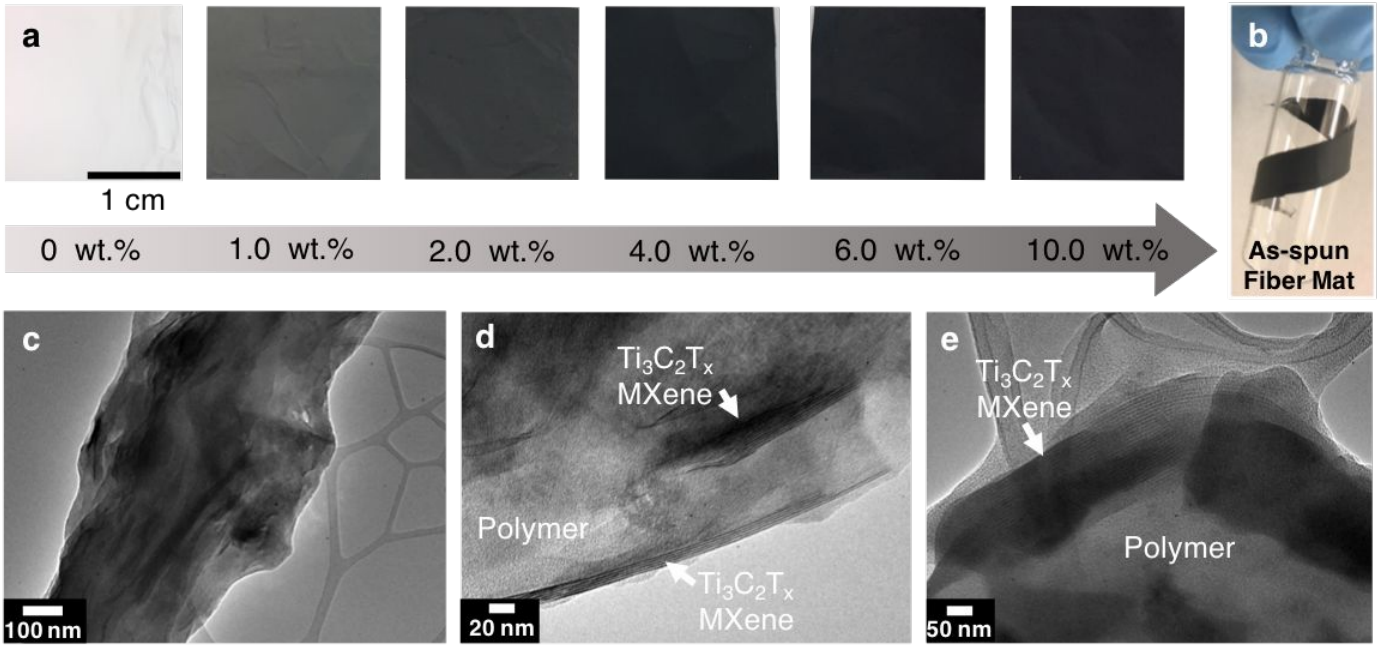

Fig. 3 a) Optical images of electrospun mats with increasing concentration of $Ti_3C_2T_x$ MXene from 0 to 10 wt.%; b) image of 10 wt.% MXene/8 wt.% PAN fibers wrapped around a vial, demonstrating the flexibility of the nanofiber mats; b) and c) TEM image of a fiber surface (as-spun) produced from a solution of 10 wt.% MXene/8 wt.% PAN, showing MXene flakes inside of the fiber.; c) TEM image of the fiber cross-section.

MXene in the PAN fibers, as designated by a shift in the main mass loss starting at 280 °C for pure PAN fibers. By comparing the percentage of total weight loss of composite fiber mats at 1000 °C to that of pure PAN fiber mats at the same temperature, we can estimate the mass loading of $Ti_3C_2T_x$ MXene in the fiber mats, which is shown in Figure 2F. Based on these calculations, adding only 2 wt.% MXene into the electrospinning solution produces electrospun mats consisting of 11.6 wt.% MXene. The maximum loading achieved in the fiber mats was 35.3 wt.%, which was prepared by electrospinning a solution with 16 wt.% $Ti_3C_2T_x$ MXene and 8 wt.% PAN.

2.3 Carbonization of MXene/PAN nanofiber mats

For use as supercapacitor electrodes, the as-spun $Ti_3C_2T_x$ MXene/PAN composite fibers were subjected to heat treatments to carbonize PAN. Since heating $Ti_3C_2T_x$ MXene at higher temperatures can lead to phase transformation and formation of TiC,[33] XRD and Raman studies were conducted to determine the optimal heat treatment for carbonizing PAN, while maintaining the structure of $Ti_3C_2T_x$ MXene within the fibers. All carbonized samples were stabilized in air at 280 °C to transform PAN into the stabilized ladder structure before carbonization under Argon (Ar). The samples are labeled according to the weight percent of MXene in the electrospinning solution and the temperature and duration of the carbonization treatment. For instance, $M_{10}CNF800_1$ refers to 10 wt.% $Ti_3C_2T_x$ MXene/PAN fibers that were carbonized at 800 °C under Ar for 1 h. As shown in Figure 5A, fibers heated at 600 °C show the (002) peak of $Ti_3C_2T_x$ MXene, confirming that the layered structure of $Ti_3C_2T_x$ MXene was maintained during the carbonization treatment. However, TiC cubic is present in the fibers heated at 800 °C for 1 h. This is clear from the missing peak at 208 cm^{-1} in the Raman

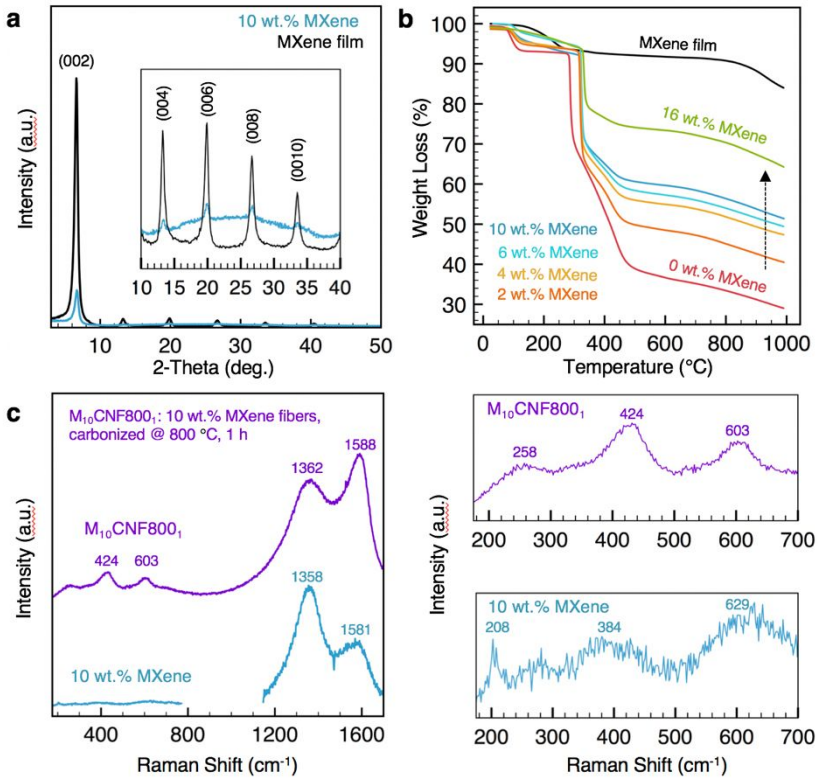

Fig. 4 a) XRD patterns of 10 wt.% $Ti_3C_2T_x$ MXene/8 wt. % PAN nanofibers (labeled 10 wt.% MXene) and a $Ti_3C_2T_x$ MXene film prepared by vacuum-assisted filtration (VAC); b) TGA curves of PAN nanofibers with various loadings of $Ti_3C_2T_x$ MXene in the electrospinning solution (0 wt.% $Ti_3C_2T_x$ MXene to 16 wt.% $Ti_3C_2T_x$ MXene in the electrospinning solution); c) Raman spectra of 10 wt.% $Ti_3C_2T_x$ MXene/8 wt.% PAN nanofibers before (labeled 10 wt.% MXene) and after carbonization at 800 °C for 1 h (labeled $M_{10}CNF800_1$), λ = 633 nm for as-spun samples, and 488 nm for carbonized samples. Right panels show magnified spectra.

spectra[34] (Figure 4C) and the formation of peaks at 36.1°, (111) peak, and 41.9°, (200) peak, in the XRD spectra (Figure 5A).[35] These peaks begin to emerge after heating the fiber mats at 700 °C for 1 h. These results are in agreement with previous works on the thermal stability of $Ti_3C_2T_x$, which show that Ti_3C_2 sheets are stable up to 800 °C under Ar atmosphere, with only small quantities of TiC and TiO_2 present and a disappearance of surface functional groups (-OH and -F).[35,36]

As shown in Figure 5B, the fibers remain intact after the heat treatment, with no noticeable fiber breakage. For all mats, the average fiber diameter decreased after carbonization. For example, the average fiber diameter decreased from 179±33 nm to 116±20 nm for pure PAN fibers carbonized at 800 °C and from 499±94 nm to 420±83 nm for *$M_{10}CNF600_1$* electrodes. Composite fiber electrodes maintain their flexibility after carbonization, as shown in Figure 5C, which demonstrates their potential application in wearable devices.

2.3 Electrochemical characterization of MXene/carbon nanofiber mats

The electrochemical behavior of the electrospun fibers was analyzed in a three-electrode setup using 1 M sulfuric acid (H_2SO_4) as the electrolyte. Nyquist plots for fibers undergoing various heat treatments are shown in Figure 6A. There are distinct differences between electrodes in both the high and low frequency regimes. In the high frequency regime, the most noteworthy difference is between the pure-carbon fibers ($CNF800_1$) and the 10 wt.% $Ti_3C_2T_x$ MXene composite fibers heated at 800 °C for 1 h ($M_{10}CNF800_1$) (inset, Figure 6A). The diameter of the semicircle dictates the resistance of ions as the migrate at the interface of the electrode and electrolyte phases. The pure-carbon fibers show a larger semi-circle in this region, indicating greater charge transfer resistance for this electrode than the composite electrode, $M_{10}CNF800_1$. The lack of any noticeable semi-circle in the high frequency regime of the $M_{10}CNF800_1$ fibers indicates that there is little to no charge transfer resistance. The low frequency regime reveals that pure carbon fibers possess faster ion transport than the composite fibers, as indicated by the slope of the straight line. This is likely due to two factors. First, ions cannot diffuse through MXene flakes, only around them, resulting in slower ion diffusion. Second, significant differences in fiber diameter may influence the diffusion kinetics. Comparing the composite fibers carbonized at different temperatures (600, 700, and 800 °C), electrodes carbonized at higher temperatures have faster ion diffusion due to smaller fiber diameter and increased conductivity of carbon and MXene after heat treatment. Additionally, electrodes carbonized for longer durations,

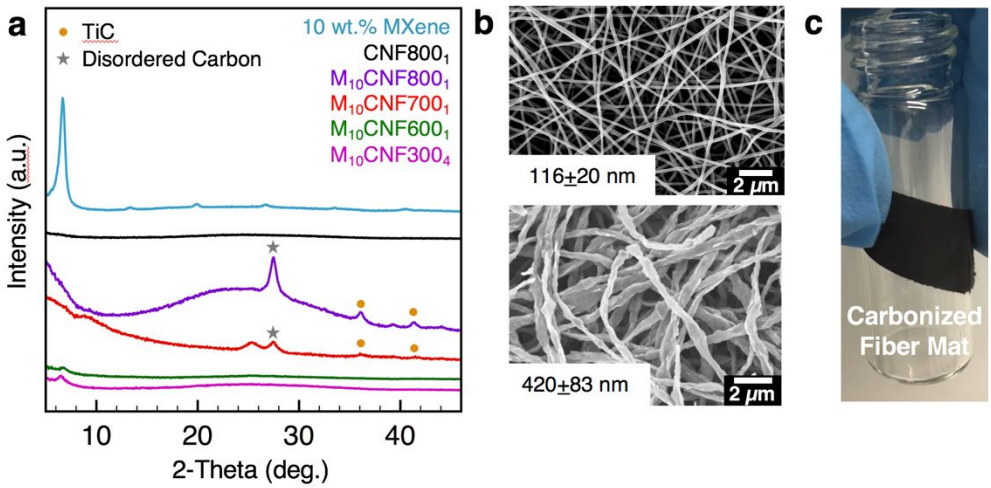

Fig. 5 a) XRD patterns of $Ti_3C_2T_x$ MXene composite fibers before and after carbonization treatments; b) SEM image of 8 wt.% PAN fibers carbonized at 800 °C for 1 h (top), and 10 wt.% $Ti_3C_2T_x$ MXene/8 wt.% PAN fibers carbonized at 600 °C for 1 h ($M_{10}CNF600_1$) (bottom); c) image of 10 wt.% $Ti_3C_2T_x$ MXene/8 wt.% PAN fibers carbonized at 700 °C for 1 h ($M_{10}CNF700_1$) wrapped around a vial, demonstrating the flexibility of the fiber mat after carbonization.

6 h instead of 1 or 2 h, show faster ion diffusion and lower resistance.

Representative cyclic voltammograms (CVs) of the composite fiber electrodes are shown in Figure 6B. From the shape of the CV profiles at 5 mV s^{-1}, it is clear that higher carbonization temperatures and longer durations leads to a more rectangular CV. Electrodes carbonized at 700 °C (Figure 6C) and above, or 600 °C for 6 h, show rectangular curves. It is important to note that the voltage window of these composite electrodes, -0.3 – 0.6 V (Figure S3A), is different than that of pure $Ti_3C_2T_x$ MXene electrodes. $Ti_3C_2T_x$ MXene electrodes typically operate between -0.7 V-0.3 V in a three-electrode set-up in an aqueous electrolyte with Ag/AgCl as the reference electrode.[9] We hypothesize that for these composite nanofibers, carbon provides protection, allowing the electrodes to operate at a higher positive potential. These results are similar to previous works on MXene/carbon composites, including MXene/rGO wet-spun fibers, which operated between 0-0.8 V in 1 M H_2SO_4 with Ag/AgCl as the reference electrode.[11] The highest areal capacitance, 239 mF/cm^2 at 10 mV/s, was achieved with fibers carbonized at 800 °C for 1 h (the fibers containing TiC). The capacitance of pure carbon fiber mats carbonized under the same conditions reached 75 mF/cm^2 at 10 mV/s. All of the fiber electrodes outperformed pure carbon fiber mats at low scan rates (Figure 6D).

To better understand the kinetics of the electrodes and the charge storage mechanisms, *b*-values were obtained at different potentials. The charge stored in an electrode material can be separated into two distinct components, a non-diffusion limited component (b = 1) and a diffusion-controlled component (b = 0.5). The capacitive component is due to the adsorption of ions and faradaic charge-transfer processes with exposed surface atoms. The diffusion-controlled component is due to diffusion-controlled intercalation processes. The relationship between the current (i) and the scan rate (v) is given by the power law

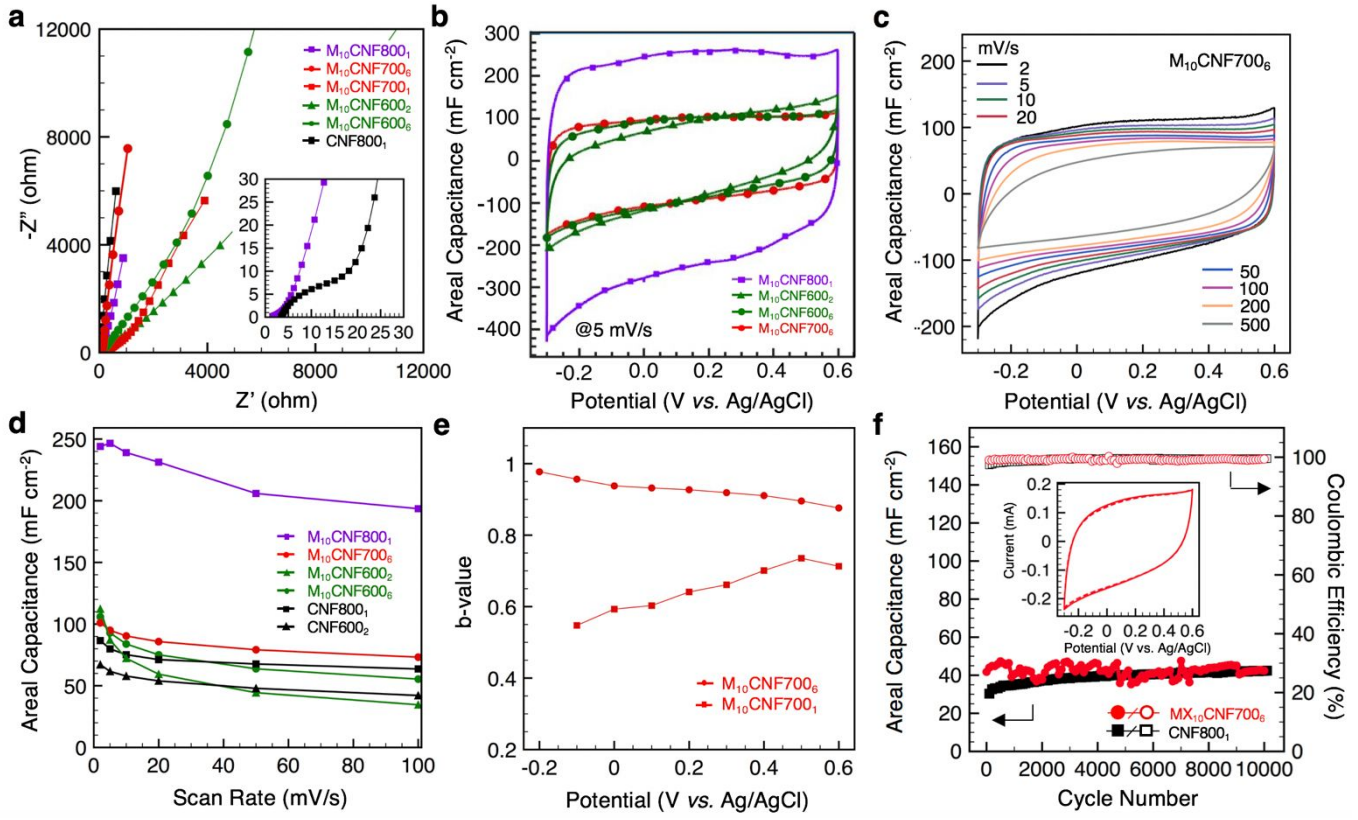

Fig. 6 a) Nyquist plot of $Ti_3C_2T_x$ MXene composite fiber electrodes and pure carbon electrodes after various carbonization treatments; b) Representative cyclic voltammograms (CVs) of the composite electrodes; c) CV curves of $M_{10}CNF700_6$ fibers at different scan rates; d) rate handling plot; e) variation of b-value with potential for fibers undergoing different heat treatments; f) long cycling. Inset shows the of $MX_{10}CNF_7700_6$ at cycle 1 (solid line) and cycle 10,000 (dashed line).

$$i=av^b; \quad (1)$$

where a and b are adjustable parameters. The b-value is obtained by plotting log(i) versus log(v). The b-values for mats carbonized at 700 °C for 1 h and 6 h are shown in Figure 6E. The b-values are above 0.9 for all potentials below 0.5 V for mats carbonized for 6 h, indicating the mechanism of charge storage is predominately not diffusion controlled. However, mats carbonized at this temperature for only 1 h show b-values 0.5-0.75 V. This indicates that samples carbonized for longer durations at 700 °C provide superior rate capability. The $MX_{10}CNF700_6$ electrode and a pure carbon electrode ($CNF800_1$) were cycled for 10,000 cycles, revealing stable performance at 50 mV/s (Figure 6F). The composite fibers remain intact after cycling (Figure S3B). It was observed that the testing environment (temperature and humidity) greatly affected the cycling performance of the electrodes (Figure S3C). Thus, the electrodes were tested under constant environmental conditions to eliminate this effect.

Comparison between the capacitance of these MXene composite fibers and corresponding literature is shown in Figure S4B and Table S2. Considering the high specific mass of MXene/CNFs relative to pure CNFs, the gravimetric capacitance was much lower for the composite fibers than pure CNFs. However, for wearable applications, areal capacitance is more practical. Compared with MXene-coated electrospun PCL fibers,[9] these composite fibers have twice the areal capacitance at 10 mV/s. The areal capacitance of $M_{10}CNF800_1$ at 10 mV/s is also twice that of carbide-derived carbon nanofelts prepared by electrospinning TiC followed by carbothermal reduction (239 mF/cm^2 and 110 mF/cm^2, respectively).[15]

3 Conclusion

We have demonstrated a simple method to incorporate $Ti_3C_2T_x$ MXene into carbon nanofiber mats. Using electrospinning as the fiber production method and optimizing heat treatments, MXene flakes were embedded into carbon nanofibers to produce freestanding fiber mats with high surface area. When employed as a binder-free electrode for supercapacitors, higher areal capacitance is achieved in comparison to pure carbon nanofibers. The electrodes exhibit areal capacitance of up to 244 mF/cm^2. While electrospinning of $Ti_3C_2T_x$ MXene is a promising method for incorporating MXene flakes into nanoscale fibers for wearable energy storage devices, it is expected that MXene-based nanofibers will have applications beyond energy storage, including filtration and electrocatalysis.

4 Experimental section

4.1 $Ti_3C_2T_x$ MXene synthesis

To selectively etch Al from Ti_3AlC_2, 3 g of Ti_3AlC_2 MAX phase (Carbon-Ukraine) with mesh size ~ ≤ 45 μm was slowly added to 60 mL of etchant containing a mixture of 9 M HCl, 49% HF, and deionized water in a volumetric ratio of 6:1:3. The solution was stirred on hot plate for 24 h. The multilayer $Ti_3C_2T_X$ MXene was washed repeatedly with deionized water by centrifugation at 3500 rpm until the pH reached neutral. Next, $Ti_3C_2T_X$ MXene was delaminated using 1 g of LiCl in 50 mL of water and stirred for 4 h. The solution was washed repeatedly with deionized water by centrifugation at 3500 rpm and the product was collected. To use it for electrospinning, the solvent (deionized water) was exchanged with dimethylformamide (DMF) by repeated centrifugation (five washes) at 9000 rpm.

4.2 Electrospinning solution preparation

Colloidal solutions of $Ti_3C_2T_x$ MXene in DMF were probe sonicated for 4 h at an amplitude of 50% and pulse ratio of 80:20. After sonication, the solutions were centrifuged at 9000 rpm for 20 min and the $Ti_3C_2T_x$ MXene sediment was collected. The sediment was added to 8 wt.% PAN in DMF to produce solutions with the MXene concentrations up to 20 wt.%. Solutions were stirred overnight at room temperature until PAN was fully dissolved.

4.3 Fabrication of MXene/PAN nanofibers and carbonization procedure

Electrospinning solutions were loaded into a plastic syringe and capped with a 21 G metal needle. A positive voltage (10-20 kV) was applied to the needle tip and a copper collector plate covered with aluminum foil was grounded. The distance between the needle tip and the collector ranged from 8-12 cm, and the infusion rate was between 0.3 – 1 mL h^{-1}. All samples were electrospun

below 30% relative humidity. The resulting electrospun mats were either used as-spun or carbonized. Samples that were carbonized were first stabilized in air at 280 °C for 1 h at a ramp rate of 5 °C min^{-1} and subsequently carbonized under Argon at a ramp rate of 5 °C min^{-1} at various temperatures (up to 800 °C) for up to 6 h.

4.4. Characterization

SEM images were taken with a field emission scanning electron microscope (FESEM Zeiss VP5 Supra) equipped with energy dispersive X-ray (EDX) spectroscopy. Fiber samples were sputter coated with platinum/palladium at 40 mA for 40 s (Cressington Scientific 108 Auto, Watford, UK) before imaging. ImageJ Software was used to measure fiber diameter. Fifty fibers were measured for each sample and the average fiber diameter was reported. Structure of the composite fibers was analyzed using transmission electron microscopy (TEM) (JEOL-2100, Japan) at an accelerating voltage of 120 kV. The X-ray diffraction (XRD) spectra were acquired using a powder diffractometer (Rigaku Smart Lab, USA) with Cu Kα radiation at a step size of 0.03° with 0.5 s dwelling time. All samples were dried at ambient temperatures before characterization. Raman spectroscopy was performed using a Renishaw in-Via Raman confocal microscope with air-cooled CCD detector. The magnification used was 50x and the laser wavelength was 633 nm for carbonized samples and 488 for as-spun samples. Spectra were collected with acquisition time of 120 s 3 times. Thermal gravimetric analysis (TGA) was performed on an SDT Q600 (TA Instruments) in Helium at a heating rate of 10 °C min^{-1} to analyze the thermal stability of the samples. MXene flake size was analyzed using Dynamic Light Scattering (Zetasizer Nano ZS, Malvern Instruments) and averaged over five measurements.

4.5 Electrochemistry

Electrochemical tests (CV, electrochemical impedance spectroscopy, and electrochemical cycling) were conducted using a VMP3 electrochemical workstation (BioLogic, France) in a three-electrode set-up with 1 M sulfuric acid (H_2SO_4) as the electrolyte. Electrospun mats and silver/silver chloride (Ag/AgCl) in 3.5 M KCl were used as the working and reference electrodes, respectively. Activated carbon (~ 100 μm thick) was used as the counter electrode. Glassy carbon was used as the current collector for the working electrode and the counter electrode. A polypropylene membrane (Celgard, USA) was used as the separator. Electrochemical impedance spectroscopy (EIS) was performed in the frequency range of 200 kHz to 10 mHz at open circuit potential by applying a sinusoidal potential signal with an amplitude of 10 mV. The areal capacitance was calculated by integrating the discharge current of the cyclic voltammograms with respect to time, according to the following equation

$$C\ (\mathrm{mF\ cm^{-2}}) = (\int_0^t i dt)/(V \times A); \qquad (2)$$

where C is the specific capacitance normalized to the geometric area of the electrode, t is the discharge time, i is the discharge current (mA), V is the voltage window, and A is the area of the electrode (cm^2), measured using ImageJ Software. For reporting the gravimetric capacitance (F g^{-1}), the specific capacitance was normalized to the mass of the entire electrode.

Conflicts of interest

There are no conflicts to declare.

Acknowledgements

This research is supported by the National Science Foundation Graduate Research Fellowship under Grant No. DGE-1646737. Any opinion, findings, and conclusion or recommendations expressed in this material are those of the author(s) and do not necessarily reflect the reviews of the National Science Foundation. SEM and TEM analyses were performed at the Core Research Facilities (CRF) of Drexel University.

Notes and references

1 B. Anasori, M. R. Lukatskaya and Y. Gogotsi. 2D metal carbides and nitrides (MXenes) for energy storage. *Nat. Rev. Mater.*, 2017, **2,** 16098.

2 X. Zhang, Z. Zhang and Z. Zhou. MXene-based materials for electrochemical energy storage. *J. Energy Chem.,* 2018, **27,** 73–85.

3 M. Naguib, V.N. Mochalin, M.W. Barsoum and Y. Gogotsi. 25th Anniversary Article: MXenes: A New

Family of Two-Dimensional Materials. *Adv. Mater.,* 2014, **26,** 992–1005.

4 C. Zhang, B. Anasori, A. Seral-Ascaso, S.H. Park, N. McEvoy, A. Shmeliov, G.S. Duesberg, J.N. Coleman, Y. Gogotsi and V. Nicolosi. Transparent, Flexible, and Conductive 2D Titanium Carbide (MXene) Films with High Volumetric Capacitance. *Adv. Mater.* 2017, **29,** 1702678.

5 K. Hantanasirisakul, M.Q. Zhao, P. Urbankowski, J. Halim, B. Anasori, S. Kota, C.E. Ren, M.W. Barsoum and Y. Gogotsi. Fabrication of $Ti_3C_2T_x$ MXene Transparent Thin Films with Tunable Optoelectronic Properties. *Adv. Electron. Mater.* 2016, **2,** 1600050

6 Y.Y. Peng, B. Akuzum, N. Kurra, M.Q. Zhao, M. Alhabeb, B. Anasori, E.C. Kumbur, H.N. Alshareef, M.D. Ger and Y. Gogotsi. All-MXene (2D titanium carbide) solid-state microsupercapacitors for on-chip energy storage. *Energy Environ. Sci.* 2016, **9,** 2847–2854.

7 F. Shahzad, M. Alhabeb, C.B. Hatter, B. Anasori, S.M. Hong, C.M. Koo and Y. Gogotsi. Electromagnetic interference shielding with 2D transition metal carbides (MXenes). *Science* 2016, **353,** 1137–1140.

8 K. Chaudhuri, M. Alhabeb, Z. Wang, V.M. Shalaev, Y. Gogotsi and A. Boltasseva. Highly Broadband Absorber Using Plasmonic Titanium Carbide (MXene). *ACS Photonics* 2018, **5,** 1115–1122.

9 Z. Zhou, W. Panatdasirisuk, T.S. Mathis, B. Anasori, C. Lu, X. Zhang, Z. Liao, Y. Gogotsi, and S. Yang. Layer-by-layer assembly of MXene and carbon nanotubes on electrospun polymer films for flexible energy storage. *Nanoscale* 2018, **10,** 6005–6013.

10 J. Zhang, S. Seyedin, Z. Gu, W. Yang, X. Wang and J.M. Razal. MXene: a potential candidate for yarn supercapacitors. *Nanoscale* 2017, **9,** 18604–18608.

11 S. Seyedin, E.R.S. Yanza and J.M. Razal. Knittable energy storing fiber with high volumetric performance made from predominantly MXene nanosheets. *J. Mater. Chem. A* 2017, **5,** 24076–24082.

12 E.A. Mayerberger, O. Urbanek, R.M. McDaniel, R.M. Street, M.W. Barsoum and C.L. Schauer. Preparation and characterization of polymer-$Ti_3C_2T_x$ (MXene) composite nanofibers produced via electrospinning. *J. Appl. Polym. Sci.* 2017, **134,** 45295.

13 P. Sobolčiak, A. Ali, M.K. Hassan, M.I. Helal, A. Tanvir, A. Popelka, M.A. Al-Maadeed, I. Krupa and K.A. Mahmoud. 2D $Ti_3C_2T_x$ (MXene)-reinforced polyvinyl alcohol (PVA) nanofibers with enhanced mechanical and electrical properties. *PLOS ONE* 2017, **12,** e0183705.

14 S. Seyedin, M.S. Romano, A.I. Minett and J.M. Razal. Towards the Knittability of Graphene Oxide Fibres. *Sci. Rep.* 2015, **5,** 14946.

15 V. Presser, L. Zhang, J.J. Niu, J. McDonough, C. Perez, H. Fong and Y. Gogotsi. Flexible Nano-felts of Carbide-Derived Carbon with Ultra-high Power Handling Capability. *Adv. Energy Mater.* 2011, **1,** 423–430

16 D.D. Edie and M.G. Dunham. Melt spinning pitch-based carbon fibers. *Carbon* 1989, **27,** 647–655.

17 F. Ko, Y. Gogotsi, A. Ali, N. Naguib, H. Ye, G.L. Yarng, C. Li and P. Willis. Electrospinning of Continuous Carbon Nanotube-Filled Nanofiber Yarns. *Adv. Mater.* 2003, **15,** 1161–1165.

18 K.D. Behler, A. Stravato, V. Mochalin, G. Korneva, G. Yushin and Y. Gogotsi. Nanodiamond-Polymer Composite Fibers and Coatings. *ACS Nano* 2009, **3,** 363–369.

19 Z. Zhou and X.-F. Wu. Graphene-beaded carbon nanofibers for use in supercapacitor electrodes: Synthesis and electrochemical characterization. *J. Power Sources* 2013, **222,** 410–416.

20 X. Lu, C. Wang, F. Favier, and N. Pinna. Electrospun Nanomaterials for Supercapacitor Electrodes: Designed Architectures and Electrochemical Performance. *Adv. Energy Mater.* 2016, **7,** 1601301.

21 D. Li, and Y. Xia, Electrospinning of Nanofibers: Reinventing the Wheel? *Adv. Mater.* 2004, **16,** 1151–1170.

22 K. Jost, D.P. Durkin, L.M. Haverhals, E.K. Brown, M. Langenstein, H.C. De Long, P. C. Trulove, Y. Gogotsi and G. Dion. Natural Fiber Welded Electrode Yarns for Knittable Textile Supercapacitors. *Adv. Energy Mater.* 2015, **5,** 1401286.

23 Y. Zhai, Y. Dou, D. Zhao, P.F. Fulvio, R.T. Mayes and S. Dai. Carbon materials for chemical capacitive energy storage. *Adv. Mater.* 2011, **23,** 4828–4850.

24 S.K. Nataraj, K.S. Yang, and T.M. Aminabhavi. Polyacrylonitrile-based nanofibers—A state-of-the-art review. *Prog. Polym. Sci.* 2012, **37,** 487–513.

25 C.-M. Yang, and B.-H. Kim. Highly conductive pitch-based carbon nanofiber/MnO_2 composites for high-capacitance supercapacitors. *J. Alloys Compd.* 2018, **749,** 441–447.

26 K. Maleski, V.N. Mochalin, and Y. Gogotsi. Dispersions of Two-Dimensional Titanium Carbide MXene in Organic Solvents. *Chem. Mater.* 2017, **29,** 1632–1640.

27. M.-Q. Zhao, C.E. Ren, Z. Ling, M.R. Lukatskaya, C. Zhang, K.L. Van Aken, M.W. Barsoum and Y. Gogotsi. Flexible MXene/Carbon Nanotube Composite Paper with High Volumetric Capacitnace. *Adv. Mater.* 2015, **27**, 339-345.

28 M. Ghidiu, S. Kota, J. Halim, A.W. Sherwood, N. Nedfors, J. Rosen, V.N. Mochalin and M.W. Barsoum. Alkylammonium Cation Intercalation into Ti_3C_2 (MXene): Effects on Properties and Ion-Exchange Capacity Estimation. *Chem. Mater.* 2017, **29,** 1099–1106.

29 W. Zhao, B. Yalcin, and M. Cakmak. Dynamic assembly of electrically conductive PEDOT:PSS nanofibers in electrospinning process studied by high speed video. *Synth. Met.* 2015, **203,** 107–116.

30 M. Hu, Z. Li, T. Hu, S. Zhu, C. Zhang and X. Wang. High-Capacitance Mechanism for Ti3C2Tx MXene by in Situ Electrochemical Raman Spectroscopy Investigation. *ACS Nano* 2016, **10,** 11344–11350.

31 M. Mariano, O. Mashtalir, F.Q. Antonio, W.-H. Ryu, B. Deng, F. Xia, Y. Gogotsi and A.D. Taylor. Solution-processed titanium carbide MXene films examined as highly transparent conductors. *Nanoscale* 2016, **8,** 16371–16378.

32 O. Mashtalir, M.R. Lukatskaya, A.I. Kolesnikov, E. Raymundo-Pinero, M. Naguib, M.W. Barsoum and Y. Gogotsi. The effect of hydrazine intercalation on the structure and capacitance of 2D titanium carbide (MXene). *Nanoscale* 2016, **8,** 9128–9133.

33 M. Alhabeb, K. Maleski, B. Anasori, P. Lelyukh, L. Clark, S. Sin and Y. Gogotsi. Guidelines for Synthesis and Processing of Two-Dimensional Titanium Carbide ($Ti_3C_2T_x$ MXene). *Chem. Mater.* 2017, **29,** 7633–7644.

34 B.H. Lohse, A. Calka and D. Wexler. Raman spectroscopy sheds new light on TiC formation during the controlled milling of titanium and carbon. *J. Alloys Compd.* 2007, **434–435,** 405–409.

35 Z. Li, L. Wang, D. Sun, Y. Zhang, B. Liu, Q. Hu and A. Zhou. Synthesis and thermal stability of two-dimensional carbide MXene Ti_3C_2. *Mater. Sci. Eng. B* 2015, **191,** 33–40.

36 K. Wang, Y. Zhou, W. Xu, D. Huang, Z. Wang and M. Hong. Fabrication and thermal stability of two-dimensional carbide Ti_3C_2 nanosheets. *Ceram. Int.* 2016, **42,** 8419–8424.

Table of Contents

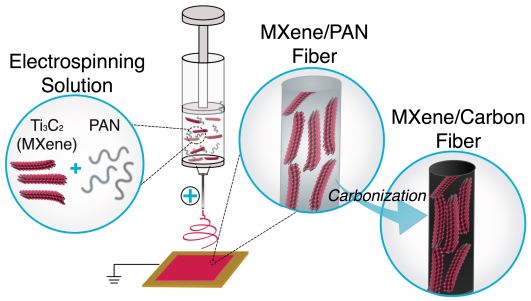

MXene/carbon composite electrodes with high loadings of MXene were prepared *via* electrospinning. These flexible and free-standing electrodes exhibit high areal capacitance relative to pure carbon nanofibers and MXene-coated fibers and textiles.